

A Heparin Binding Motif Rich in Arginine and Lysine is the Functional Domain of YKL-40



Nipaporn Ngernyuang^{*,†}, Wei Yan[‡],
Lawrence M. Schwartz[‡], Dennis Oh[§], Ying-bin Liu[¶],
Hongzhuan Chen^{*} and Rong Shao^{*,‡,¶}

^{*}Department of Pharmacology, Shanghai Jiao Tong University School of Medicine, 280 South Chongqi Road, Shanghai, China 200092; [†]Chulabhorn International College of Medicine, Thammasat University, Pathum Thani, Thailand 12120;

[‡]Department of Biology, Morrill Science Center South, University of Massachusetts, Amherst, USA 01003; [§]Department of Surgery, Baystate Medical Center, School of Medicine, University of Massachusetts, USA 01199; [¶]The Key laboratory of Shanghai and Department of General Surgery, Shanghai Jiao Tong University, School of Medicine, 1665 Kongjiang Road, Shanghai, China 200092

Abstract

The heparin-binding glycoprotein YKL-40 (CHI3L1) is intimately associated with microvascularization in multiple human diseases including cancer and inflammation. However, the heparin-binding domain(s) pertinent to the angiogenic activity have yet been identified. YKL-40 harbors a consensus heparin-binding motif that consists of positively charged arginine (R) and lysine (K) (RRDK; residues 144–147); but they don't bind to heparin. Intriguingly, we identified a separate KR-rich domain (residues 334–345) that does display strong heparin binding affinity. A short synthetic peptide spanning this KR-rich domain successfully competed with YKL-40 and blocked its ability to bind heparin. Three individual point mutations, where alanine (A) substituted for K or R (K337A, K342A, R344A), led to remarkable decreases in heparin-binding ability and angiogenic activity. In addition, a neutralizing anti-YKL-40 antibody that targets these residues and prevents heparin binding impeded angiogenesis in vitro. MDA-MB-231 breast cancer cells engineered to express ectopic K337A, K342A or R344A mutants displayed reduced tumor development and compromised tumor vessel formation in mice relative to control cells expressing wild-type YKL-40. These data reveal that the KR-rich heparin-binding motif is the functional heparin-binding domain of YKL-40. Our findings shed light on novel molecular mechanisms underlying endothelial cell angiogenesis promoted by YKL-40 in a variety of diseases.

Neoplasia (2018) 20, 182–192

Introduction

YKL-40, also known as human cartilage glycoprotein-39 (HCGP39) or chitinase-3-like-1 (CHI3L1), is a 40-kDa secreted glycoprotein that consists of 383 amino acids [1–3]. As a member of glycoside hydrolase family 18, YKL-40 binds to chitin-like oligosaccharides, but surprisingly it fails to function as either a chitinase or a hydrolase. The failure to observe this enzymatic activity is ascribed to a mutation in the chitinase-3-like catalytic domain in which an essential glutamic acid is replaced with a leucine [1,2]. As a result, YKL-40 functional domains remain to be determined. YKL-40 is normally expressed by cells in variety of tissues, including chondrocytes [3] and synoviocytes [4] in bone, vascular smooth muscle cells [5] in blood vessels, and macrophages [6] and neutrophils [7] in the immune system. However, its biophysiological function is incompletely understood.

YKL-40 was previously shown to possess high binding affinity for heparin [2,3,5], the property that is essential for its ability to induce tumor angiogenesis in many cancers [8]. In this regard, it resembles other heparin-binding proteins that require the presence of heparin to

Address all correspondence to: Rong Shao, Ph.D., Department of Pharmacology, Shanghai Jiao Tong University School of Medicine, Shanghai, China 200025.

E-mail: rongshao@sjtu.edu.cn

Received 18 September 2017; Revised 20 November 2017; Accepted 20 November 2017

© 2018 The Authors. Published by Elsevier Inc. on behalf of Neoplasia Press, Inc. This is an open access article under the CC BY-NC-ND license (<http://creativecommons.org/licenses/by-nc-nd/4.0/>). 1476-5586

<https://doi.org/10.1016/j.neo.2017.11.011>

mediate tumor growth and angiogenesis, including growth factors (e.g. HGF, bFGF, EGF, VEGF), cytokines (e.g. IL-8), and extracellular matrix proteins (e.g. vitronectin, fibronectin, laminin, thrombospondin) [9–12]. Indeed, YKL-40 harbors a consensus heparin-binding motif [arginine (R), R, aspartate (D), lysine (K), BBXB; B: basic amino acid residue, X: hydrophobic residue] located in residues 144–147, which implicates this core element in the ability to bind heparin. However, intriguing evidence obtained from an X-ray crystallographic analysis demonstrated that the RRDK motif does not possess the ability to bind to heparin [2], meaning that the location of the heparin-binding motif(s) within YKL-40 is currently unknown.

Growing clinical evidence has indicated that expression of YKL-40 is aberrant in a number of human diseases including type 2 diabetes [13], obesity and insulin resistance in children [14], Alzheimer's diseases [15], heart failure [16] and other cardiovascular disorders [17]. In addition, YKL-40 plays an active role in a vast array of inflammatory diseases that involve bacterial infections [18], rheumatoid arthritis [19], osteoarthritis [20], hepatic fibrosis and hepatitis [21], asthma and chronic obstructive pulmonary diseases [22], neuroinflammation [23], and bowel lesions [24]. Although the molecular mechanisms underlying these inflammatory disorders are largely unknown, it has been postulated that YKL-40 is associated with both substantial remodeling of extracellular matrix and extensive infiltration and differentiation of macrophages, the primary leukocytes in response to inflammation. Studies with YKL-40 deficient mice provide strong evidence supporting this hypothesis, as these mice exhibited noticeably compromised antigen-induced Th2 inflammation and impaired macrophage activation and differentiation [25]. In addition, YKL-40 was also found to drive the proliferation and survival of fibroblastic cells, a process that is central to tissue injury and wound repairing [26].

Over the past decades it has emerged that serum levels of YKL-40 can serve as a diagnostic and prognostic cancer biomarker. Multiple independent clinical trials have demonstrated a robust correlation between elevated serum levels of YKL-40 and reduced cancer survival in a variety of human carcinomas, including breast cancer, colorectal cancer [27], ovarian cancer [28], leukemia, lymphoma [29], and glioblastoma [30]. We discovered that YKL-40 acts as an angiogenic factor to induce blood vessel formation in these cancers, thus establishing the key pathologic signature that mediates tumor progression [8]. However, the primary molecular mechanism that accounts for heparin binding capacity of YKL-40 is poorly understood. Therefore, the identification and characterization of a heparin-binding motif within YKL-40 will provide novel mechanistic insights into its active role in the pathogenesis of a wide range of human diseases, as well as define a potential therapeutic target for functional intervention.

Materials and Methods

Point Mutation of YKL-40

Single arginine or lysine point mutations were generated by PCR-based site-directed mutagenesis according to manufacturer's instruction of a kit (Fisher Scientific Inc). In brief, a single point mutation was designed in one of 5'-phosphorylated primers and linear PCR product containing the desired mutation was generated using YKL-40 wide type DNA as a template. The PCR product was then circularized with Quick T4 DNA Ligase. The resulting plasmid was transformed into competent JM109 *E. coli* cells (Promega Inc). The final mutated constructs were validated by DNA sequencing.

Generation of Recombinant YKL-40

The full-length His-tag cDNA encoding wild type, point-mutated, or GFP-fused YKL-40 was subcloned into pFastBac1 vector (Invitrogen, CA). Following transformation and amplification in DH10Bac *E. coli*, bacmid DNA containing different versions of the YKL-40 gene was transfected into Sf9 insect cells by using CellFECTIN reagent (Invitrogen) and baculoviral medium was produced. A Ni-NTA column was used to purify recombinant YKL-40 according to manufacturer's instruction (Invitrogen, Piscataway, NJ, USA) and pure YKL-40 was finally isolated through a PD-10 desalting column (Amersham Biosciences).

Heparin-Sepharose Affinity Binding Assays and Competitive Assays

Recombinant YKL-40 or YKL-40 short peptides were loaded into a heparin-Sepharose affinity column (GE Healthcare Life Sciences) pre-equilibrated with 20 mM sodium phosphate buffer (pH 7.4) containing 25 mM NaCl. After washing with 5 volume of the equilibration buffer, the column was eluted with 20 mM sodium phosphate buffer containing 0.1, 0.25, 0.5 or 1.0 M NaCl. The samples were collected and concentrated with centrifugal concentrators prior to immunoblotting. For competitive assays, YKL-40-GFP was preloaded onto heparin-Sepharose columns, and after washing, different versions of recombinant YKL-40 competitors were added to the columns sequentially at increasing ratios (1:1, 1:4 and 1:8) and then were washed with 0.5 M NaCl to elute heparin-binding proteins.

ELISA

We used a previously described protocol to measure the heparin-binding affinity of YKL-40 mutants with some of modification [31]. In brief, heparin solution (10 µg/ml in PBS, Sigma) was pre-coated on a 96-well plate overnight at 4°C. After extensive washing and blocking with 0.2% porcine gelatin in PBST, individual recombinant mutants of YKL-40 from 4 to 500 ng were added to the wells for 2 h at room temperature followed by incubation with a biotinylated anti-YKL-40 antibody (1:100, R & D system). Streptavidin-alkaline phosphatase (1:100, Sigma Inc.) was then introduced for 1 h prior to a final addition of a substrate p-Nitrophenyl phosphate (25 mg/ml, Sigma).

Cancer Cell Lines Stably Expressing YKL-40

Full length wild type and point-mutated YKL-40 cDNA was subcloned into the retroviral pCMV-neo-vector. 293 T retroviral packaging cells were transfected with different versions of YKL-40 or vector control DNA in the presence of the pCL 10A1 vector using X-tremegene HP (Roche Inc) as the delivery vehicle. Forty-eight hours after transfection, the supernatant was harvested and filtered through 0.45-µm pore size filter and the virus-containing medium was used to infect tumor cells. Selection with 800 µg/ml of G418 was started 48 h after infection and the drug-resistant cell populations were used for subsequent studies.

Immunoprecipitation and Western blotting: Individual different versions of recombinant YKL-40 (1 µg) were mixed with 3 µl of either a mouse monoclonal antibody (mAY) or a rabbit polyclonal antibody (rAY) [32] against YKL-40 in 500 µl of immunoprecipitation buffer containing 10 mM Tris pH 7.4, 1% Triton, 0.5% NP-40, 150 mM NaCl, 20 mM NaF, 0.2 mM Na₃VO₄, 1 mM EDTA, 1 mM EGTA and 0.2 mM PMSF. The immunocomplex was

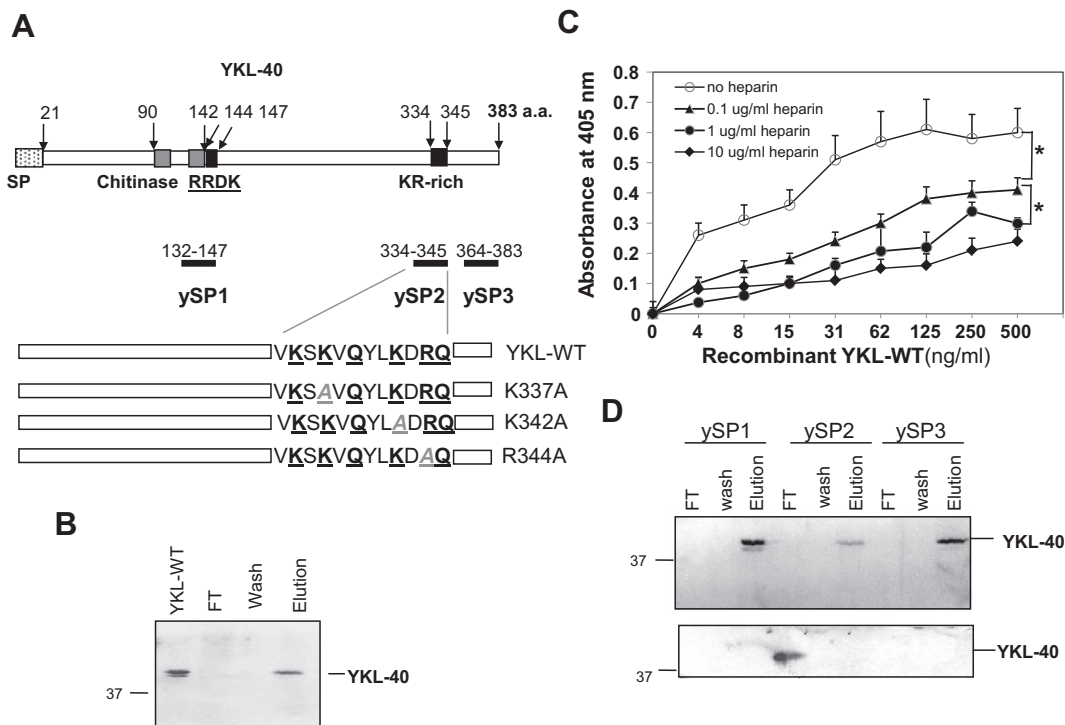


Figure 1. YKL-40 constructs, mutants and heparin-binding property. (A) The schematic drawing of YKL-WT shows a signal peptide (SP) sequence, two chitinase domains between residues 90–142, one consensus heparin-binding RRDK motif between residues 144–147, and one putative KR-rich region between residues 334–345. Three bars indicate short peptides ySP1, ySP2 and ySP3, and bottom sequences represent YKL-WT and point mutation constructs. (B) Recombinant YKL-WT (1 μ g) was used for a heparin-Sepharose affinity-binding assay. YKL-WT was eluted with 1 M NaCl (the last lane). The first lane indicates a positive YKL-WT control and the second lane contains the flow-through (FT). (C) Competitive binding assay with heparin. Recombinant YKL-WT was pre-mixed with heparin (0, 0.1, 1 or 10 μ g/ml) for 30 min prior to introduction to the plate pre-coated with heparin for YKL-40 ELISA. Heparin-binding affinity was measured with absorbance at 405 nm. N = 4. * P < .05 compared with YKL-WT in the absence or presence of 0.1 μ g/ml heparin. (D) ySP1, ySP2, or ySP3 (10 μ g) was used for YKL-WT (1 μ g) competitive heparin-binding assays. 1 M NaCl was used to elute final heparin-binding YKL-WT. A fraction of FT and wash buffer and whole concentrated elution were measured for YKL-WT (top blot) and the rest fractions of FT and wash buffer were concentrated and assayed for YKL-WT levels (bottom blot) using immunoblotting.

incubated with protein A sepharose CL-4B (GE Healthcare Life Sciences) at 4°C for 4 h followed by extensive washing. The samples were then subjected to immunoblotting using mAY or rAY as described previously [8].

Tube Formation Assays

HMVEC (2×10^4 cells) were transferred onto 96-well Matrigel in the presence of different versions of recombinant YKL-40 (200 ng/ml) (Becton Dickson Lab, Bedford, MA). After 12 hours of incubation, tube-forming structures were analyzed as described previously [8].

Migration Assays

HMVEC (2×10^5 cells) were pre-incubated with serum-free medium for 12 h and then transferred onto transwells (24-well plates) pre-coated with collagen IV (100 μ g/ml). The lower chamber of transwells included different versions of YKL-40 (200 ng/ml). After 4 hours of incubation, cells in the top chamber of the transwells membrane were removed using Q-tip. Average number of cells that migrated through the membrane was calculated from five different fields in each sample.

Wound Healing Assay

HMVECs were grown to confluency in a 24-well dish. A plastic tip was used to make a scratch cross through the well. Cultured medium

was changed to serum-free medium in the presence of different versions of recombinant YKL-40. 24 h later, movement of the cells into the scratched space was analyzed under a microscope.

Tumor xenografts in mice

All animal experiments were performed under Institutional Animal Care and Use Committee approval of University of Massachusetts Amherst. MDA-MB-231 cells (1.5×10^6) expressing different versions of YKL-40 in 100 μ l of PBS were injected subcutaneously into 4-week old female SCID/Beige mice. Tumor growth from these injected cells was monitored weekly and calculated as follows: volume = length \times width² \times 0.52.

Immunohistochemistry

Tumors were excised and cryosectioned to 6 μ m thickness prior to processing for immunostaining with anti-YKL-40 and anti-CD31 antibodies. In brief, the samples were incubated in 3% H₂O₂ to block endogenous peroxidase activity for 30 min followed by incubation with blocking buffer containing 10% goat serum for 1 h at room temperature. The rAY (1:400) or a rat anti-CD31 monoclonal antibody (1: 500, BD Pharmagen, Mountain View, CA, USA) was incubated at room temperature for 2 h and a goat anti-rabbit or rat secondary antibody (1: 100) conjugated with HRP was then added.

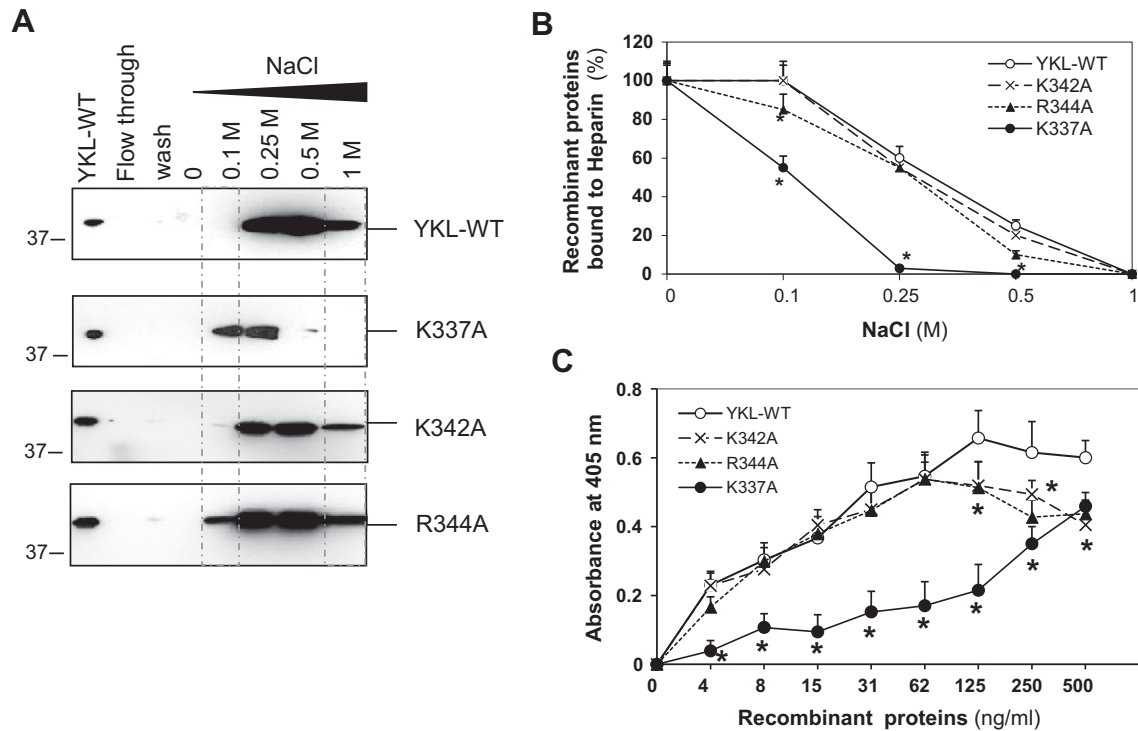


Figure 2. Lysine or arginine mutations of the C-terminal KR-rich domain led to decreased heparin-binding affinity of YKL-40. (A) Recombinant mutants (10 μ g) were individually loaded onto a heparin-Sepharose column (0.5 ml). After washing, a concentration gradient of NaCl as indicated was applied to the column. All of flow through, wash buffer, and eluted fractions were used to measure YKL-40 levels. The first lane is recombinant YKL-WT as a positive control in immunoblotting. An additional elution with 1 M NaCl following the last elution did not show any YKL-40 remained in the column (data not shown). (B) Density of the bands shown in "A" was quantitatively analyzed using ImageJ software. The concentration of the protein was measured at each concentration of NaCl and was compared to the total cross-over protein level which was set up as 100%. N = 3. (C) Different mutants of YKL-40 were tested for their abilities to bind to heparin using an ELISA. Heparin binding of YKL-WT and individual mutants was dose-dependent. N = 3. * $P < .05$ compared with corresponding concentrations of YKL-WT.

Finally, DAB substrate (Dako Inc., Carpinteria, CA, USA) was introduced for several minutes and after washing, methyl green will be used for counterstaining.

Statistics

Data are expressed as mean \pm SE and "N" refers to the numbers of individual experiments performed. Differences among groups were determined using one-way ANOVA analysis followed by the Newman-Keuls test. The 0.05 level of probability was used as the criterion of significance.

Results

YKL-40 is a heparin-binding glycoprotein that contains both a consensus heparin-binding motif (RRDK) in residues 144–147 and a KR-rich domain in residues 334–345 proximal to the C-terminus that may function to bind heparin (Figure 1A). Interestingly, a previous study focusing on the crystal structure of YKL-40 demonstrated that the consensus RRDK motif does not possess binding affinity for heparin [2]. Thus we reasoned that the alternative C-terminal KR-rich domain likely plays a central role in the heparin-binding activity. To test this hypothesis, we first measured binding affinity of YKL-40 with heparin using a heparin-Sepharose affinity binding assay. Recombinant wild-type YKL-40 (YKL-WT) displayed the ability to bind to heparin in a Sepharose-beads column, but was fully dissociable from the column following exposure to a

high concentration of NaCl (Figure 1B). YKL-WT bound heparin in a dose-dependent manner, and pre-treatment with free heparin also dose-dependently prevented YKL-WT from binding to heparin coated on plates (Figure 1C), confirming that YKL-40 is a heparin-binding protein.

To discriminate between the consensus RRDK motif and the KR-rich domain as potential heparin binding sites, we employed three short synthetic peptides in a competitive heparin-binding assay, where ySP1, ySP2, and ySP3 were designated for the consensus RRDK motif, KR-rich domain, and C-terminus, respectively (Figure 1A). Notably, ySP2 displayed strong heparin-binding affinity that competed efficiently against YKL-WT and reduced its ability to bind to the column (Figure 1D). In contrast, neither ySP1 nor ySP3 displayed this capacity, implicating that the C-terminal KR-rich domain is a key element contributing to the heparin binding.

The C-terminal KR-rich domain of YKL-40 harbors a cluster of multiple basic amino acids such as one R and three K residues (Figure 1A) [33,34]. To determine if these basic residues contribute to heparin binding, we created three point mutation constructs of YKL-40, in which alanine (A) substituted for the K or R of K337, K342 and R344 individually to generate K337A, K342A and R344A, respectively (Figure 1A). These three recombinant mutants were subsequently evaluated for heparin binding capacity in the presence of a concentration gradient of NaCl. As shown in Figs. 2A and B, YKL-WT was eluted from the column by sequential concentrations

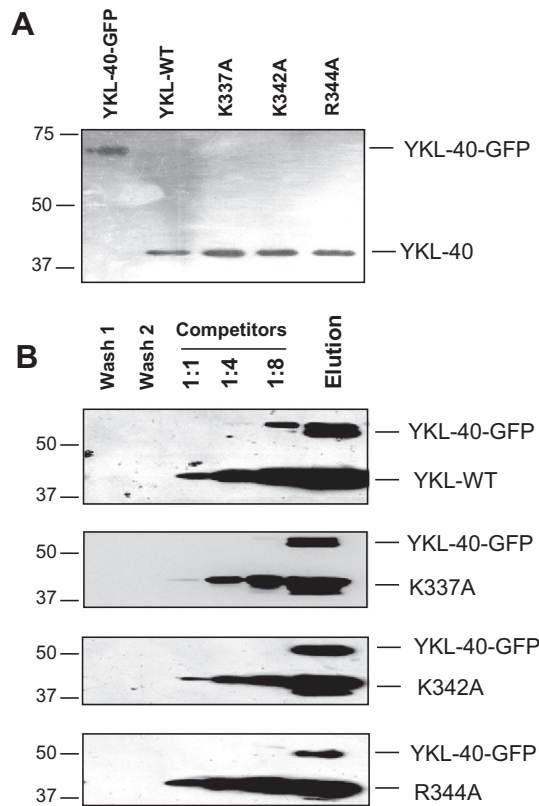


Figure 3. Lysine or arginine mutations of the C-terminal KR-rich domain reduced the ability of mutant YKL-40 to compete with YKL-WT for heparin binding. (A) YKL-WT fused with GFP displayed a higher molecular mass than different mutant versions of YKL-40 in an immunoblotting assay, but are still recognized by rAY. (B) YKL-WT-GFP was preloaded onto each heparin-Sepharose column and after wash, different versions of YKL-40 (YKL-WT, K337A, K342A, R344A) as competitors from 1:1, 1:4, to 1:8 ratio were added to the columns and NaCl (0.5 M) was used for final elution.

of NaCl from 0.25 to 1.0 M, but K337A was eluted by lower concentrations of NaCl (between 0.1 and 0.25 M). K342A displayed the heparin-binding affinity similar to YKL-WT, while R344A demonstrated the binding affinity between K337A and K342A (Figs. 2A & B). These mutants were also tested for their heparin-binding affinities using ELISA (Figure 2C). In concert with the earlier results from the heparin column binding assays, each mutant displayed the ability to bind heparin in a dose-dependent manner with the highest heparin-binding affinity displayed by YKL-WT followed by K342A and R344A at concentrations above 62 ng/ml, while K337A exhibited the lowest affinity. These results suggest that the rank of heparin-binding affinity for these mutants is YKL-WT > K342A > R344A > K337A.

To further confirm that these point mutations result in distinct heparin-binding capacities, we evaluated the ability of these recombinant mutants to compete against YKL-WT. In order to distinguish YKL-WT from the mutants on immunoblots, YKL-WT was fused with green fluorescent protein (GFP) which increased the apparent molecular weight by 26 kDa (Figure 3A). However, this fusion modification did not influence its heparin-binding affinity, since the binding activities of YKL-WT-GFP and YKL-WT were identical (data not shown). To fully saturate the affinity-binding capacity of heparin-Sepharose columns (Supplemental Figure 1),

YKL-WT-GFP (0.5 mg protein/ml beads) was loaded onto the columns first and then YKL-WT or individual mutants with different concentrations were applied (Figure 3B). An 8-fold excess of YKL-WT relative to YKL-WT-GFP could partially displace YKL-WT-GFP from the column, whereas none of the mutants could effectively compete for heparin binding (Figure 3B), even in the presence of a 10-fold higher concentration than YKL-WT-GFP (data not shown). This underscores the high binding affinity of YKL-40 for heparin. Thus, these data support the previous findings that the K337, K342 and R344 within the C-terminal KR-rich domain of YKL-40 act as critical elements for heparin binding.

YKL-40 is a potent angiogenic factor that is able to promote endothelial cell-initiated vascularization at concentrations between 50–250 ng/ml in vitro [8,32]. To determine if the mutations of K337, K342 and R344 alter the angiogenic activities of YKL-40, we evaluated the ability of these mutant proteins (200 ng/ml) to form endothelial cell-mediated vascular tubes in Matrigel. Relative to the control cultures, exogenous YKL-WT protein induced a 1.8-fold increase in human microvascular endothelial cells (HMVEC) tube formation (Figs. 4A & B). In contrast, none of recombinant K337A, K342A, and R344A mutant proteins could enhance the formation of vascular networks, which is consistent with their lower heparin-binding affinity than YKL-WT (Figure 2C). In addition, none of these proteins altered HMVEC proliferation during a 24-h period (data not shown). In agreement with the tube formation data, none of these mutant proteins enhanced HMVEC motility either in cell migration (Figure 4C) or wound healing assays (Figure 4D). These data strongly support the hypothesis that the C-terminal KR-rich motif required for heparin binding is essential for the angiogenic activity of YKL-40.

We previously created and characterized a neutralizing monoclonal anti-YKL-40 antibody (mAY) from mice and a polyclonal anti-YKL-40 (rAY) from rabbits [32]. Given previous evidence that mAY can block YKL-40-induced angiogenesis [32,35], we reasoned that the mAY likely binds to a domain in YKL-40 that is essential for its physiological activity. To test this hypothesis, we first performed an immunoblotting assay using mAY and rAY (Figure 5A). While mAY bound to all versions of YKL-40, there was variable binding when these basic amino acid residues were individually mutated. We quantified this interaction and observed that the relative binding affinity appears to be: YKL-WT >> K342A > R344A > K337A (Figure 5A). In contrast to mAY, the rAY revealed equal ability to bind all of these different versions of YKL-40, since the antibody was generated from rabbits immunized with ySP3, the peptide encoding a non-functional region of YKL-40. To further verify that the mAY binding is specific for the C-terminal KR-rich motif, we mutated an arginine R145 to a glycine (R145G) in the consensus RRDK motif and then evaluated its ability to bind to mAY (Figure 5B). Unlike the other mutants, R145G did not alter its association with mAY as compared with YKL-WT. The R145G mutant protein was just as effective as YKL-WT at inducing HMVEC tube formation (Figure 5C), thus verifying that it retains full physiological activity. These data support the hypothesis that K337, K342 and R344 of the C-terminal RK-rich domain are the unique sites for mAY binding.

To further probe different levels of the interaction between mAY and the various versions of mutants, we performed immunoprecipitation followed by immunoblotting. The data we observed suggest that the relative binding affinity of mutants with mAY was YKL-WT > K342A > R344A > K337A, whereas there was no

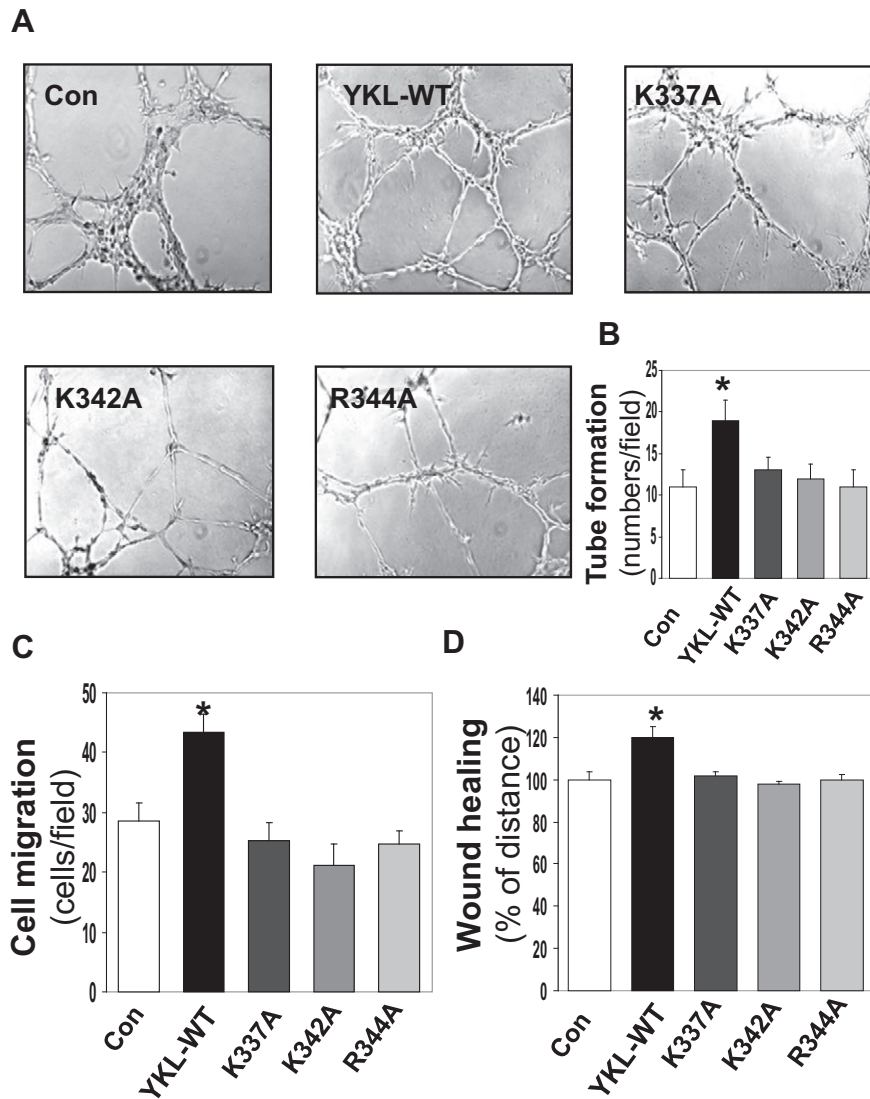


Figure 4. Angiogenic activity of YKL-40 requires the presence of the lysine and arginine residues within the RK-rich domain. Recombinant YKL-WT, K337A, K342A, and R344A (200 ng/ml) were added to HMVECs in Matrigel. Tube formation was analyzed overnight (A). The tubes from in A were quantified (B). $N = 3$. * $P < .05$ compared with HMVECs treated with serum-free medium only. Different recombinant YKL-40 proteins were used for cell migration (C) and wound healing assays (D) as described in the Methods. $N = 3-4$ * $P < .05$ compared with HMVECs treated with serum-free medium only.

binding difference between YKL-WT and different mutants of YKL-40 with rAY (Figure 5D). Thus, the binding between YKL-40 mutants and mAY paralleled the heparin-binding signatures for the mutants as found earlier (Figure 2), highlighting that the KR-rich heparin-binding motif of YKL-40 is the functional domain. Next, to determine if mAY binding to the KR-rich heparin-binding site can prevent YKL-40 from binding to heparin, we incubated YKL-40 with mAY first and then loaded onto a heparin-Sepharose column. Pre-binding of YKL-40 to mAY (1:1 ratio) reduced YKL-40 binding to heparin (Figs. 6A & B). When mAY was increased to ten-fold greater than YKL-40 (1:10 ratio), mAY markedly inhibited YKL-40 binding to heparin, as the large portion of YKL-40 was observed in flow through, whereas YKL-40 retained in elution was minimal. In contrast, mIgG treatment failed to block YKL-40 binding to heparin (Figs. 6A & B). To further validate neutralizing activity of mAY, we exploited HMVECs for cell motility in the presence and absence of mAY. As shown in Figure 6C, mAY abrogated the YKL-40-induced

cell migration to the basal levels, whereas rAY did not have the ability to promote cell motility, consistent with the data observed with these mutant proteins (Figure 4A). Collectively, all of the results suggest that mAY blocks YKL-40-induced angiogenesis through binding to K337, K342 and/or R344 of the KR-rich heparin-binding domain.

In an attempt to determine if these secreted versions of the YKL-40 mutants by cancer cells can recapitulate the activities of recombinant proteins identified earlier, we engineered MDA-MB-231 breast cancer cells to individually express each of the mutant genes (Figure 7A). The conditioned media from these cultures were transferred to HMVECs for tube formation assays. In agreement with the data obtained with the recombinant proteins (Figure 4), the conditioned medium from MDA-MB-231 cells expressing YKL-WT, but not those expressing these versions of mutants, significantly augmented tube formation (Figure 7B). These data support the notion that an intact C-terminal KR-rich domain of YKL-40 is required for its physiological activity and any loss of these basic residues (K337, K342 or R344) within this motif fails to retain the activity.

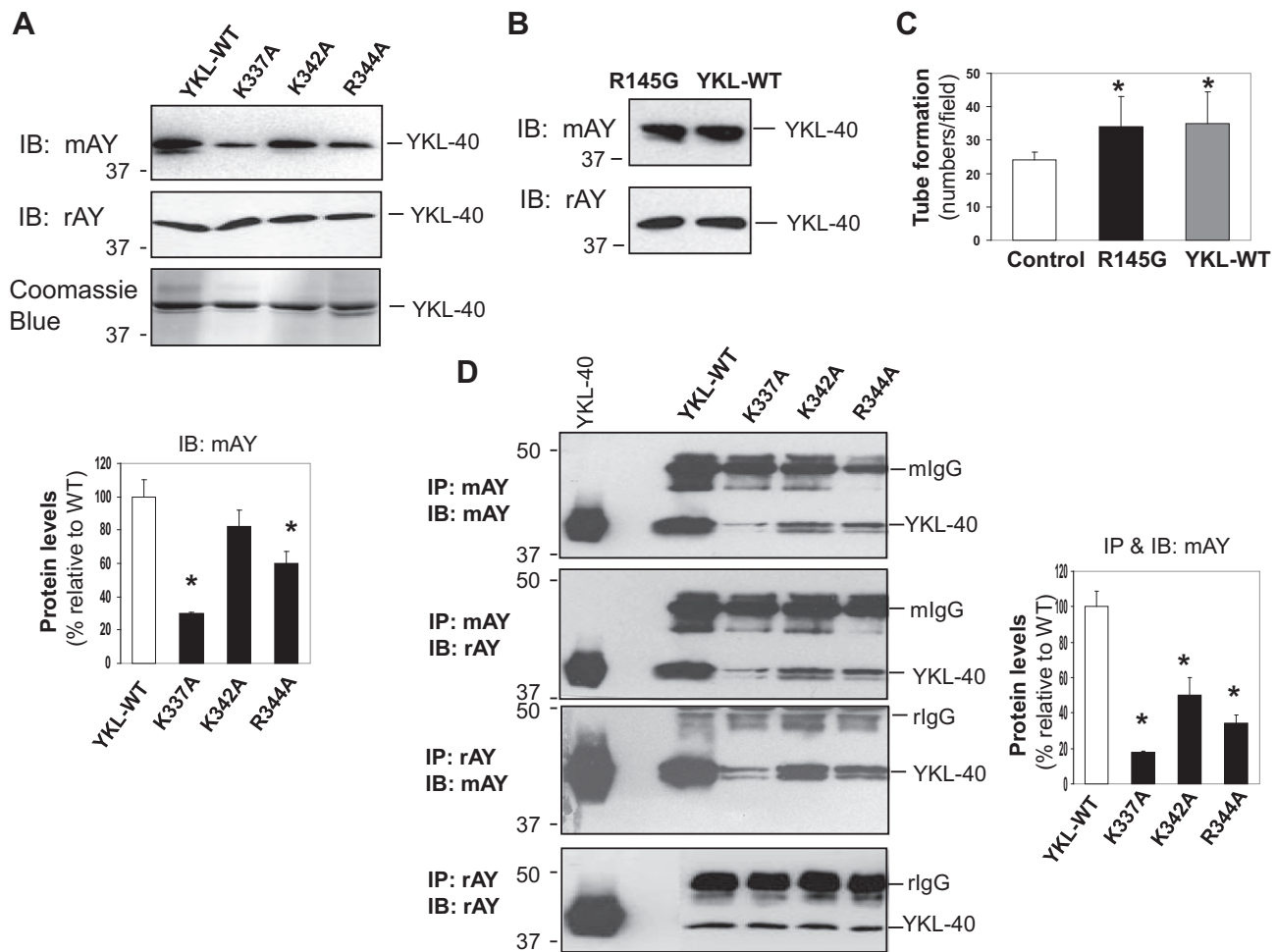


Figure 5. mAY, but not rAY, binds and blocks YKL-40 via its recognition of lysine and arginine residues within the KR-rich domain. (A) Equal amount of each recombinant YKL-WT, K337A, K342A, and R344A was subjected to immunoblotting using mAY and rAY. Coomassie blue staining was also used to demonstrate that there was equal samples loading. The intensity of the bound protein bands shown in immunoblotting using mAY was quantified. $N = 3$, $*P < .05$ compared with YKL-WT. (B) YKL-WT and R145G (200 ng/ml) were subjected for immunoblotting using mAY and rAY. (C) Recombinant YKL-WT and R145G (200 ng/ml) were used to test tube formation of HMVECs. $N = 3$, $*P < .05$ compared with HMVECs treated with serum-free medium only as a control. (D) Equal amount of each recombinant YKL-WT, K337A, K342A, and R344A was immunoprecipitated with either mAY or rAY followed by immunoblotting using either mAY or rAY. The first lane is the recombinant YKL-40 as a positive control in immunoblotting. One representative of quantified protein intensity from the top-three blots was shown. $N = 3$, $*P < .05$ compared with YKL-WT.

To determine if these YKL-40 point-mutations alter tumor angiogenesis and tumor development in vivo, we performed xenografts within SCID/Beige mice with MDA-MB-231 cells expressing YKL-WT or each of the different mutants. All of these animals formed palpable tumors beginning about week 8 after transplantation. By week 12, mice receiving YKL-WT cells developed tumors that were approximately 5-fold larger than those observed in animals bearing control MDA-MB-231 cells (Figure 7C). All of the other mutant-bearing tumors were significantly smaller than those developed from YKL-WT-expressing cells. While tumors derived from R344A-expressing cells were similar in size to those generated from control cells, the ones developed from cells expressing the K337A and K342A mutants were evidently suppressed to 20–45% of tumor size seen with control cells. These in vivo data are inconsistent with in vitro evidence that K337A, K342A, and R344A slightly enhanced cell proliferation by 10–20% relative to control

MDA-MB-231 or ones expressing YKL-WT (Supplemental Figure 2). This suggests that none of these mutant forms of YKL-40 predisposes the cells toward acceleration of tumor growth in vivo. Instead, their ability to inhibit angiogenesis in vitro may be the determinant responsible for tumor growth in vivo. To test directly this hypothesis, we analyzed these tumors with immunohistochemistry using an anti-CD31 antibody that specifically recognizes vascular endothelial cells (Figure 7D). Quantitative analysis indicated that blood vessels in the YKL-WT tumors were 2-fold more abundant than those developed from MDA-MB-231 control cells. Interestingly, the blood vessel density of R344A tumors was comparable to that seen in controls. In agreement with the diminished tumor volume (Figure 7C), the blood vessel density in the tumors derived from K337A and K342A cells was reduced to 35–40% of that found in the controls, suggesting that these mutants impede tumor development via a paracrine inhibition in endothelial cell-mediated angiogenesis. In

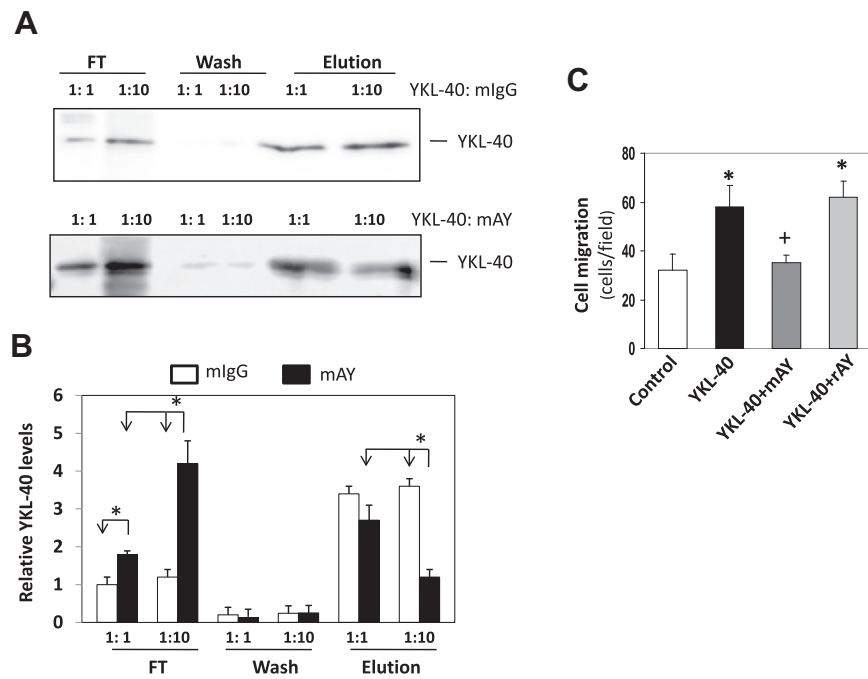


Figure 6. Pre-binding of mAY to YKL-40 blocks its heparin binding and mAY inhibits YKL-40 activity. (A) YKL-40 was pre-incubated with mlgG or mAY (1: 1 or 1: 10 molar ratio) overnight at 4°C. The complex samples were then loaded onto heparin-Sepharose columns as described in the Methods. Following wash, the eluted samples were used for immunoblotting. (B) The images shown in A were quantitatively analyzed. N = 3. * $P < .05$ compared with 1:1 mlgG, 1:1 mAY or 1:10 mlgG. The density of 1:1 mlgG flow through (FT) was set up as 1 unit. (C) HMVECs were used for cell migration assay as described in the Methods in the presence of mlgG (10 μ g/ml, control), YKL-40 (200 ng/ml + mlgG), mAY (10 μ g/ml), or rAY (10 μ g/ml). N = 3, * P and + $P < .05$ compared with control and YKL-40, respectively.

an analysis of tumor distant metastasis, mice transplanted with the different engineered tumor cells did not exhibit ectopic tumor dissemination with the exception of one mouse (out of six) that received YKL-WT cells and developed pulmonary metastasis (Supplemental Figure 3).

To evaluate expression of YKL-40 in these tumors, we performed immunohistochemistry with rAY rather than mAY, because the latter reduced YKL-40 mutant protein binding activity. While tumors developed from control cells expressed low levels of endogenous YKL-40 (Figure 7E), the tumors derived from engineered lines consistently expressed high levels of their engineered YKL-40 protein. Co-immunofluorescence analysis of the control tumors showed that the YKL-40-expressing cells were also positive for smooth muscle alpha actin (SMa), a marker of vascular smooth muscle cells or pericytes but negative for F4/80, a macrophage marker (Supplemental Figure 4). These data suggest that the endogenous, non-tumor derived YKL-40 is mainly produced from vascular smooth muscle cells.

Taken together, the in vitro and in vivo data presented here all support our hypothesis that the C-terminal KR-rich domain of YKL-40 binds heparin and that this domain is required for the pro-angiogenic properties of YKL-40.

Discussion

While YKL-40 is a member of glycoside hydrolase family 18 that is capable of binding chitin-like oligosaccharides, it lacks chitinase/hydrolase activity due to the mutation of glutamic acid in the chitinase-3-like catalytic domain [1,2]. Likewise, YKL-40 is also a heparin-binding glycoprotein that contains a consensus heparin-binding

motif (BBXB); but this domain does not bind heparin. Consequently, the functional domains responsible for the biological and pathophysiological properties of YKL-40 are still enigmatic. In the current study, we have employed multiple molecular and cellular biological methods, including biochemical, immunological and pharmacological approaches, to identify the functional element responsible for the ability of YKL-40 to bind heparin and drive pathological processes such as tumor angiogenesis. To our knowledge this is the first study to unveil the KR-rich domain of the C-terminus, rather than the typical RRDK domain, as a functional domain responsible for heparin binding and biological function of YKL-40. The identification of this KR-rich motif has significantly advanced our understanding of a new distinct heparin-binding motif for YKL-40 in vascular biology, and also provides a potential target for therapeutic intervention in treating a wide type of human diseases.

A wealth of evidence has established the paradigm that the heparin-binding capacity is of paramount importance in the pathological activities of a wide range of heparin-binding proteins that include angiogenic factors (bFGF, EGF, VEGF), cytokines (IL-8), and extracellular matrix proteins (vitroectin, fibronectin, laminin, thrombospondin), all of which mediate tumorigenesis, chronic inflammation and other diseases [36,37]. Consistent with these factors, the ability of YKL-40 to bind heparin at high affinity is considered to be a core factor in its ability to trigger vascular endothelial cell angiogenesis [8]. The angiogenic activity of YKL-40 can be fully eliminated, if the heparan sulfate groups on endothelial cell surface are removed by pre-treating the cells with heparitinase and chondroitinase ABC, since they prevent YKL-40 from the binding to cell membrane [8]. In concert with these studies, impairing

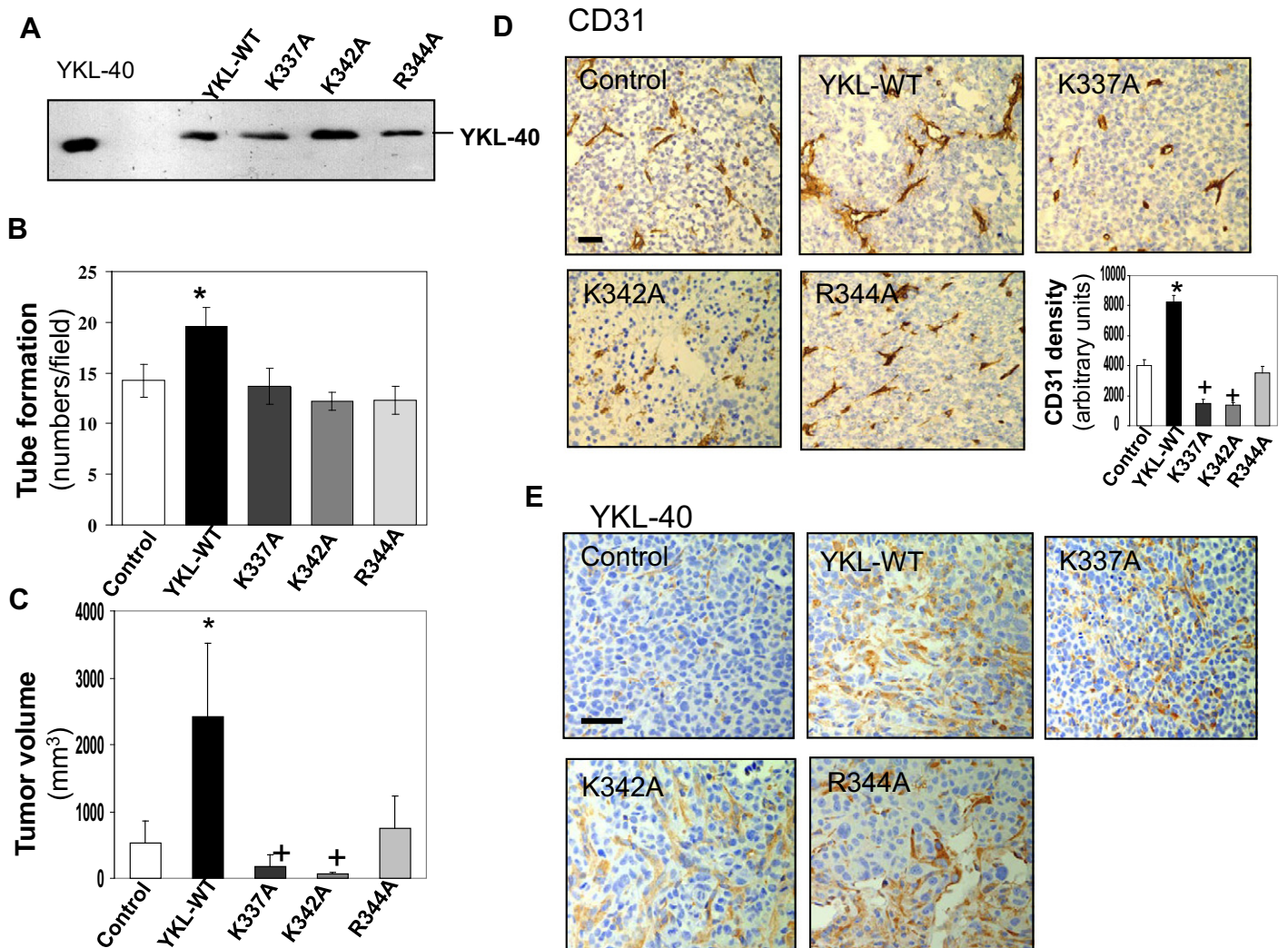


Figure 7. Tumor development and angiogenesis induced by the breast cancer cell line MDA-MB-231 expressing ectopic different YKL-40 mutants. MDA-MB-231 cells were engineered to ectopically express different forms of YKL-40 mutants. After 48 h of incubation in serum-free medium, the expression of secreted YKL-40 proteins was measured using immunoblotting (A) or assayed for their ability to induce tube formation in HMVECs (B). These cells were transplanted into SCID/Beige mice as described in the Methods. Tumor volume was measured weekly and the final results at week 12 were quantified (C). Tumor samples were subjected to IHC with an anti-CD31 antibody (D) or rAY (E). Quantification of vessel density based on CD31 staining was analyzed using NIH ImageJ software. N = 5. **P* and +*P* < .05 relative to controls. Bars: 100 μ m.

heparin-binding activity by mutations of K337, K342 and R344 in the KR-rich domain of YKL-40 led to loss of the ability to induce angiogenesis in cultured endothelial cells. Furthermore, the mouse xenograft studies presented here offer key *in vivo* evidence to establish the functional role of these basic residues in YKL-40-induced tumor angiogenesis.

The heparin binding affinity of YKL-40 can be partially diminished by γ SP2 or with an 8 to 10-fold higher concentration of YKL-40 itself, but not by the other mutants or other short synthetic peptides tested. The three recombinant YKL-40 mutants we generated displayed dissimilar levels of heparin-binding affinity (K342A > R344A > K337A), but the potential mechanisms under these functional differences have not been fully determined. We speculate that it is likely associated with their 3-D structural organization characterized by the divergent positions of basic amino acids in the KR-rich domain, particularly for K337 and K342, which exhibit drastic difference in their ability to bind heparin. Interestingly, while there was a modest decrease in the heparin-binding affinities of

K342A and R344A as compared with YKL-WT, they nevertheless display a remarkable suppression of angiogenesis both *in vitro* and *in vivo*, thus demonstrating the importance of these basic amino acid residues in the biological and pathological activity of YKL-40. Although an additional K335 located in this RK-rich domain has yet to be characterized, it is conceivable that K335 may play the same role as the other two K337 and K342 in the heparin-binding property and the resulting pathophysiological activity of YKL-40. Chen et al., have reported that a chitin-binding motif that resides within residues 325–339 is pivotal for pro-survival activity of YKL-40 on colonic epithelial cells [38,39]. However, they did not identify individual residues within this domain that might mediate this function. It is plausible that K335 and/or K337 at least partially contribute to the YKL-40-induced cell survival activity in their studies. In context with these data, the current study has demonstrated the importance of these basic amino acid residues of the KR-rich domain in biological and pathological activity of YKL-40.

One of the intriguing observations from our in vivo studies was that both YKL-40 K337A and K342A-expressing tumor cells substantially restricted tumorigenesis and angiogenesis relative to either the R344A mutant or non-engineered control tumor cells. Although their low heparin binding affinity may partially contribute to the in vivo results, the substantial mechanism that mediates this striking difference is currently unknown. It is worth speculating that K337A and K342A mutants may also antagonize the activity of the endogenous YKL-40 derived from vascular pericytes, thereby significantly inhibiting the production of endothelial cell-derived tumor vessels. Indeed, the role of pericyte derived YKL-40 in tumor angiogenesis was established recently [40]. It would be valuable to determine if inhibiting pericyte-derived YKL-40 (e.g. with mAY) results in an angiogenesis-compromised phenotype identical to that was found in the tumors derived from K337A or K342A expressing cells.

Over the past two decades, emerging data have demonstrated that serum levels of YKL-40 are elevated in a broad arrange of human diseases including cancer, liver injury, asthma, diabetes, chronic inflammation, and cardiac disorders [13,17,21]. Furthermore, the increased concentrations of YKL-40 in cancer are positively correlated with the disease severity such as cancer metastasis and decreased patient survival, suggesting that serum levels of YKL-40 can serve as a clinically useful biomarker for both cancer diagnosis and prognosis. However, efforts to develop a clinical regimen aiming at YKL-40 in cancer have been considerably hampered, possibly owing to lack of substantially mechanistic insights into its structural elements that mediate its angiogenic signature. Therefore, the identification of the KR-rich functional domain of YKL-40 may represent a viable target for clinical intervention for the development of new drugs that can target the individual basic amino acid residues. In support of this contention, binding of mAY with YKL-40 was found at these specific residues, thus preventing heparin binding and inhibiting YKL-40 activity. The data were consistent with our previous reports demonstrating that mAY abrogated tumor angiogenesis both in vitro and in animal trials [32,35]. Hence, we have provided crucial evidence to support our hypothesis that the KR-rich heparin-binding motif may serve as a novel and effective target as an anti-angiogenic therapy in a variety of solid tumors and other diseases.

Funding

This work was supported by National Science Foundation China No. 81772512, translational research funds BJ17000176110 from Shanghai Jiao Tong University School of Medicine and research scientists' incubation funds from Shanghai Jiao Tong University Xinhua Hospital JZPI201716 (RS).

Conflict of Interest

Authors claim no any conflict of interest present in this study.

Appendix A. Supplementary data

Supplementary data to this article can be found online at <https://doi.org/10.1016/j.neo.2017.11.011>.

References

- [1] Renkema GH, Boot RG, Au FL, Donker-Koopman WE, and Strijland A, et al (1998). Chitotriosidase, a chitinase, and the 39-kDa human cartilage glycoprotein, a chitin-binding lectin, are homologues of family 18 glycosyl hydrolases secreted by human macrophages. *Eur J Biochem* **251**, 504–509.
- [2] Fusetti F, Pijning T, Kalk KH, Bos E, and Dijkstra BW (2003). Crystal structure and carbohydrate-binding properties of the human cartilage glycoprotein-39. *J Biol Chem* **278**, 37753–37760.
- [3] Hu B, Trinh K, Figueira WF, and Price PA (1996). Isolation and sequence of a novel human chondrocyte protein related to mammalian members of the chitinase protein family. *J Biol Chem* **271**, 19415–19420.
- [4] Nyirkos P and Golds EE (1990). Human synovial cells secrete a 39 kDa protein similar to a bovine mammary protein expressed during the non-lactating period. *Biochem J* **269**, 265–268.
- [5] Shackleton LM, Mann DM, and Millis AJ (1995). Identification of a 38-kDa heparin-binding glycoprotein (gp38k) in differentiating vascular smooth muscle cells as a member of a group of proteins associated with tissue remodeling. *J Biol Chem* **270**, 13076–13083.
- [6] Rehli M, Krause SW, and Andreesen R (1997). Molecular characterization of the gene for human cartilage gp-39 (CHI3L1), a member of the chitinase protein family and marker for late stages of macrophage differentiation. *Genomics* **43**, 221–225.
- [7] Zurawska-Plaksej E, Lugowska A, Hetmanczyk K, Knapik-Kordecka M, and Piwowar A (2015). Neutrophils as a Source of Chitinases and Chitinase-Like Proteins in Type 2 Diabetes. *PLoS One* **10**, e0141730.
- [8] Shao R, Hamel K, Petersen L, Cao QJ, and Arenas RB, et al (2009). YKL-40, a secreted glycoprotein, promotes tumor angiogenesis. *Oncogene* **28**, 4456–4468.
- [9] Blanco MA and Kang Y (2011). Signaling pathways in breast cancer metastasis - novel insights from functional genomics. *Breast Cancer Res* **13**, 206.
- [10] Spillmann D, Witt D, and Lindahl U (1998). Defining the interleukin-8-binding domain of heparan sulfate. *J Biol Chem* **273**, 15487–15493.
- [11] Rapraeger AC, Krufka A, and Olwin BB (1991). Requirement of heparan sulfate for bFGF-mediated fibroblast growth and myoblast differentiation. *Science* **252**, 1705–1708.
- [12] Park PW, Reizes O, and Bernfield M (2000). Cell surface heparan sulfate proteoglycans: selective regulators of ligand-receptor encounters. *J Biol Chem* **275**, 29923–29926.
- [13] Han JY, Ma XY, Yu LJ, Shao Y, and Wang QY (2015). Correlation between serum YKL-40 levels and albuminuria in type 2 diabetes. *Genet Mol Res* **14**, 18596–18603.
- [14] Kyrgios I, Galli-Tsinopoulou A, Stylianou C, Papakonstantinou E, and Arvanitidou M, et al (2012). Elevated circulating levels of the serum acute-phase protein YKL-40 (chitinase 3-like protein 1) are a marker of obesity and insulin resistance in prepubertal children. *Metabolism* **61**, 562–568.
- [15] Kester MI, Teunissen CE, Sutphen C, Herries EM, and Ladenson JH, et al (2015). Cerebrospinal fluid VILIP-1 and YKL-40, candidate biomarkers to diagnose, predict and monitor Alzheimer's disease in a memory clinic cohort. *Alzheimers Res Ther* **7**, 59.
- [16] Harutyunyan M, Christiansen M, Johansen JS, Kober L, and Torp-Petersen C, et al (2012). The inflammatory biomarker YKL-40 as a new prognostic marker for all-cause mortality in patients with heart failure. *Immunobiology* **217**, 652–656.
- [17] Xu Y, Wang Q, Liu Y, Cui R, and Lu K, et al (2016). Association between *Helicobacter pylori* infection and carotid atherosclerosis in patients with vascular dementia. *J Neurol Sci* **362**, 73–77.
- [18] Otterdal K, Janardhanan J, Astrup E, Ueland T, and Prakash JA, et al (2014). Increased endothelial and macrophage markers are associated with disease severity and mortality in scrub typhus. *J Infect* **69**, 462–469.
- [19] Cinton C, Johansen JS, Christensen JJ, Price PA, and Sorensen S, et al (2002). High serum YKL-40 level after surgery for colorectal carcinoma is related to short survival. *Cancer* **95**, 267–274.
- [20] Vaananen T, Koskinen A, Paukkeri EL, Hamalainen M, and Moilanen T, et al (2014). YKL-40 as a novel factor associated with inflammation and catabolic mechanisms in osteoarthritic joints. *Mediators Inflamm* **2014**, 215140.
- [21] Pawlak K, Rozkiewicz D, Mysliwiec M, and Pawlak D (2013). YKL-40 in hemodialyzed patients with and without cardiovascular complications - the enhancement by the coexistence of the seropositivity against hepatitis C virus infection. *Cytokine* **62**, 75–80.
- [22] Hinks TS, Brown T, Lau LC, Rupani H, and Barber C, et al (2016). Multidimensional endotyping in patients with severe asthma reveals inflammatory heterogeneity in matrix metalloproteinases and chitinase 3-like protein 1. *J Allergy Clin Immunol* **138**, 61–75.
- [23] Hellwig K, Kvartsberg H, Portelius E, Andreasson U, and Oberstein TJ, et al (2015). Neurogranin and YKL-40: independent markers of synaptic degeneration and neuroinflammation in Alzheimer's disease. *Alzheimers Res Ther* **7**, 74.

- [24] Lee IA, Kamba A, Low D, and Mizoguchi E (2014). Novel methylxanthine derivative-mediated anti-inflammatory effects in inflammatory bowel disease. *World J Gastroenterol* **20**, 1127–1138.
- [25] Lee CG, Hartl D, Lee GR, Koller B, and Matsuura H, et al (2009). Role of breast regression protein 39 (BRP-39)/chitinase 3-like-1 in Th2 and IL-13-induced tissue responses and apoptosis. *J Exp Med* **206**, 1149–1166.
- [26] Lee CG, Da Silva CA, Dela Cruz CS, Ahangari F, and Ma B, et al (2011). Role of chitin and chitinase/chitinase-like proteins in inflammation, tissue remodeling, and injury. *Annu Rev Physiol* **73**, 479–501.
- [27] Johansen JS, Christensen IJ, Jorgensen LN, Olsen J, and Rahr HB, et al (2015). Serum YKL-40 in risk assessment for colorectal cancer: a prospective study of 4,496 subjects at risk of colorectal cancer. *Cancer Epidemiol Biomarkers Prev* **24**, 621–626.
- [28] Yip P, Chen TH, Sessaiah P, Stephen LL, and Michael-Ballard KL, et al (2011). Comprehensive serum profiling for the discovery of epithelial ovarian cancer biomarkers. *PLoS One* **6**, e29533.
- [29] Mylin AK, Abildgaard N, Johansen JS, Heickendorff L, and Kreiner S, et al (2015). Serum YKL-40: a new independent prognostic marker for skeletal complications in patients with multiple myeloma. *Leuk Lymphoma* **56**, 2650–2659.
- [30] Gallego Perez-Larraya J, Paris S, Idbaih A, Dehais C, and Laigle-Donadey F, et al (2014). Diagnostic and prognostic value of preoperative combined GFAP, IGFBP-2, and YKL-40 plasma levels in patients with glioblastoma. *Cancer* **120**, 3972–3980.
- [31] Harris EN, Baggenstoss BA, and Weigel PH (2009). Rat and human HARE/stabilin-2 are clearance receptors for high- and low-molecular-weight heparins. *Am J Physiol Gastrointest Liver Physiol* **296**, G1191–1199.
- [32] Faibish M, Francescone R, Bentley B, Yan W, and Shao R (2011). A YKL-40-neutralizing antibody blocks tumor angiogenesis and progression: a potential therapeutic agent in cancers. *Mol Cancer Ther* **10**, 742–751.
- [33] Albini A, Benelli R, Presta M, Rusnati M, and Ziche M, et al (1996). HIV-tat protein is a heparin-binding angiogenic growth factor. *Oncogene* **12**, 289–297.
- [34] Hileman RE, Fromm JR, Weiler JM, and Linhardt RJ (1998). Glycosaminoglycan-protein interactions: definition of consensus sites in glycosaminoglycan binding proteins. *Bioessays* **20**, 156–167.
- [35] Shao R, Francescone R, Ngernyuang N, Bentley B, and Taylor SL, et al (2014). Anti-YKL-40 antibody and ionizing irradiation synergistically inhibit tumor vascularization and malignancy in glioblastoma. *Carcinogenesis* **35**, 373–382.
- [36] Martino MM, Briquez PS, Ranga A, Lutolf MP, and Hubbell JA (2013). Heparin-binding domain of fibrin(ogen) binds growth factors and promotes tissue repair when incorporated within a synthetic matrix. *Proc Natl Acad Sci U S A* **110**, 4563–4568.
- [37] Xu R, Rudd TR, Hughes AJ, Siligardi G, and Fernig DG, et al (2013). Analysis of the fibroblast growth factor receptor (FGFR) signalling network with heparin as coreceptor: evidence for the expansion of the core FGFR signalling network. *FEBS J* **280**, 2260–2270.
- [38] Chen CC, Pekow J, Llado V, Kanneganti M, and Lau CW, et al (2011). Chitinase 3-like-1 expression in colonic epithelial cells as a potentially novel marker for colitis-associated neoplasia. *Am J Pathol* **179**, 1494–1503.
- [39] Chen CC, Llado V, Eurich K, Tran HT, and Mizoguchi E (2011). Carbohydrate-binding motif in chitinase 3-like 1 (CHI3L1/YKL-40) specifically activates Akt signaling pathway in colonic epithelial cells. *Clin Immunol* **140**, 268–275.
- [40] Francescone R, Ngernyuang N, Yan W, Bentley B, and Shao R (2014). Tumor-derived mural-like cells coordinate with endothelial cells: role of YKL-40 in mural cell-mediated angiogenesis. *Oncogene* **33**, 2110–2122.